

Skeletal muscle adiposity, coronary microvascular dysfunction, and adverse cardiovascular outcomes

Ana Carolina do A.H. Souza^{1†}, Amelie S. Troschel^{2,3†}, Jan P. Marquardt², Ibrahim Hadžić^{4,5}, Borek Foldyna ⁶, Filipe A. Moura¹, Jon Hainer ¹, Sanjay Divakaran ¹, Ron Blankstein¹, Sharmila Dorbala¹, Marcelo F. Di Carli¹, Hugo J.W.L. Aerts^{4,5}, Michael T. Lu⁶, Florian J. Fintelmann², and Viviany R. Taqueti ^{1*}

¹Cardiovascular Imaging Program, Brigham and Women's Hospital, Harvard Medical School, 75 Francis St., Boston, MA 02115, USA; ²Division of Thoracic Imaging, Department of Radiology, Massachusetts General Hospital, Boston, MA 02114, USA; ³Medical Department II, Klinikum Wolfsburg, Wolfsburg, Germany; ⁴Artificial Intelligence in Medicine (AIM) Program, Massachusetts General Hospital, Harvard Medical School, Boston, MA 02114, USA; ⁵Department of Radiology and Nuclear Medicine, Maastricht University Medical Center, Maastricht, The Netherlands; and ⁶Cardiovascular Imaging Research Center, Massachusetts General Hospital, Harvard Medical School, Boston, MA 02114, USA

Received 15 April 2024; revised 28 October 2024; accepted 12 November 2024

Abstract

Background and Aims Skeletal muscle (SM) fat infiltration, or intermuscular adipose tissue (IMAT), reflects muscle quality and is associated with inflammation, a key determinant in cardiometabolic disease. Coronary flow reserve (CFR), a marker of coronary microvascular dysfunction (CMD), is independently associated with body mass index (BMI), inflammation and risk of heart failure, myocardial infarction, and death. The relationship between SM quality, CMD, and cardiovascular outcomes is not known.

Methods Consecutive patients ($n = 669$) undergoing evaluation for coronary artery disease with cardiac stress positron emission tomography demonstrating normal perfusion and preserved left ventricular ejection fraction were followed over a median of 6 years for major adverse cardiovascular events (MACEs), including death and hospitalization for myocardial infarction or heart failure. Coronary flow reserve was calculated as stress/rest myocardial blood flow. Subcutaneous adipose tissue (SAT), SM, and IMAT areas (cm^2) were obtained from simultaneous positron emission tomography attenuation correction computed tomography using semi-automated segmentation at the 12th thoracic vertebra level.

Results Median age was 63 years, 70% were female, and 46% were nonwhite. Nearly half of patients were obese (46%, BMI 30–61 kg/m^2), and BMI correlated highly with SAT and IMAT ($r = .84$ and $r = .71$, respectively, $P < .001$) and moderately with SM ($r = .52$, $P < .001$). Decreased SM and increased IMAT, but not BMI or SAT, remained independently associated with decreased CFR (adjusted $P = .03$ and $P = .04$, respectively). In adjusted analyses, both lower CFR and higher IMAT were associated with increased MACE [hazard ratio 1.78 (95% confidence interval 1.23–2.58) per -1 U CFR and 1.53 (1.30–1.80) per $+10$ cm^2 IMAT, adjusted $P = .002$ and $P < .0001$, respectively], while higher SM and SAT were protective [hazard ratio .89 (.81–.97) per $+10$ cm^2 SM and .94 (.91–.98) per $+10$ cm^2 SAT, adjusted $P = .01$ and .003, respectively]. Every 1% increase in fatty muscle fraction [IMAT/(SM + IMAT)] conferred an independent 2% increased odds of CMD [CFR < 2 , odds ratio 1.02 (1.01–1.04), adjusted $P = .04$] and a 7% increased risk of MACE [hazard ratio 1.07 (1.04–1.09), adjusted $P < .001$]. There was a significant interaction between CFR and IMAT, not BMI, such that patients with both CMD and fatty muscle demonstrated highest MACE risk (adjusted $P = .02$).

* Corresponding author. Tel: +1 617 732 8667, Email: vtaqueti@bwh.harvard.edu

† The first two authors contributed equally to the study.

© The Author(s) 2025. Published by Oxford University Press on behalf of the European Society of Cardiology. All rights reserved. For commercial re-use, please contact reprints@oup.com for reprints and translation rights for reprints. All other permissions can be obtained through our RightsLink service via the Permissions link on the article page on our site—for further information please contact journals.permissions@oup.com.

Conclusions Increased intermuscular fat is associated with CMD and adverse cardiovascular outcomes independently of BMI and conventional risk factors. The presence of CMD and SM fat infiltration identified a novel at-risk cardiometabolic phenotype.

Structured Graphical Abstract

Key Question

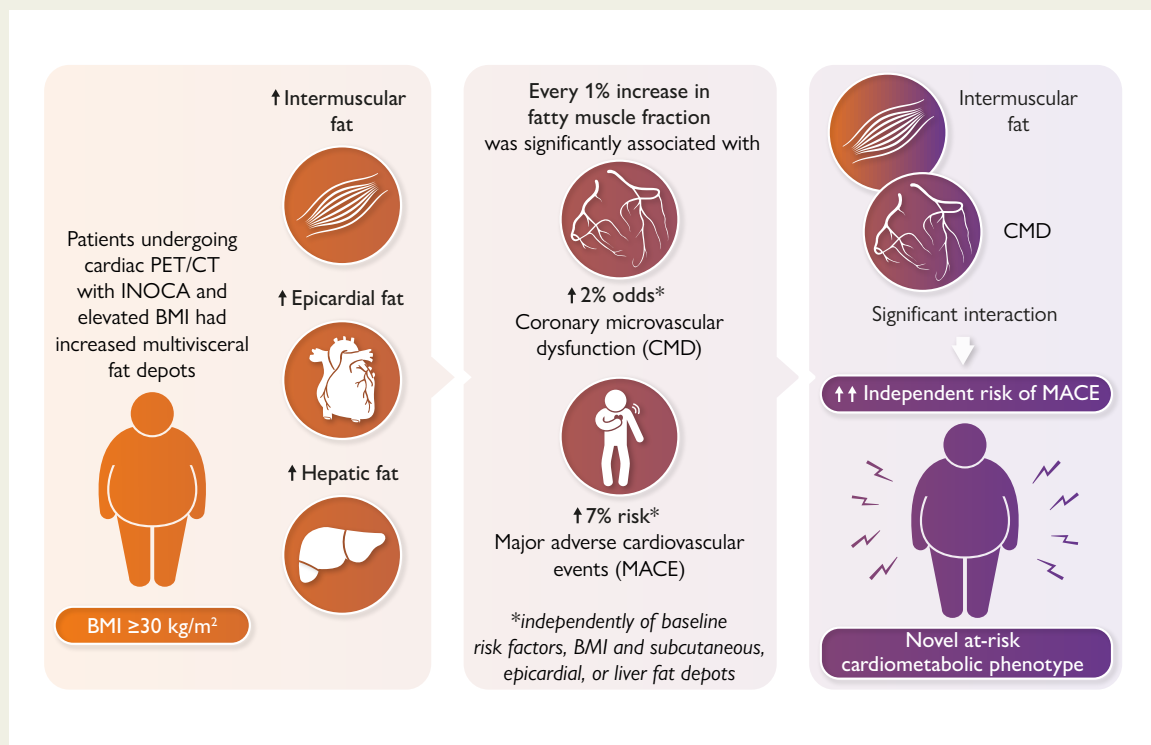
What is the independent relationship between intermuscular adipose tissue (IMAT), a novel fat depot interspersed between skeletal muscle fibers, and adverse outcomes in patients with ischaemia and no obstructive coronary artery disease (INOCA)?

Key Finding

- Intermuscular fat infiltration was associated with coronary microvascular dysfunction (CMD) and adverse cardiovascular outcomes independently of body mass index (BMI), conventional ectopic (epicardial, hepatic) fat depots, and cardiovascular risk factors.
- Every 1% increase in thoracic fatty muscle fraction conferred an independent 2% increased odds of CMD and a 7% increased risk of major adverse cardiovascular events.
- The presence of both CMD and IMAT identified a novel at-risk cardiometabolic phenotype prevalent in patients with INOCA.

Take Home Message

- Obesity-related cardiovascular risk is not well-captured by BMI, especially in those with fewer traditional risk factors and a greater proportion of subcutaneous adiposity.
- Skeletal muscle quantity and quality are tied to coronary microvascular function and identify cardiometabolic risk beyond traditional measures of visceral adiposity.



Intermuscular adiposity, a novel ectopic fat depot, is associated with coronary microvascular dysfunction independently of body mass index and other conventional risk factors, and modifies its effect on adverse cardiovascular outcomes in patients with cardiometabolic disease. BMI, body mass index; CMD, coronary microvascular dysfunction; CT, computed tomography; INOCA, ischaemia and no obstructive coronary artery disease; MACE, major adverse cardiovascular event; PET, positron emission tomography.

Keywords

Obesity • Body composition • Intermuscular fat • Coronary microvascular dysfunction • Cardiovascular events • Ischaemia and no obstructive coronary artery disease

Introduction

Overweight or obesity is prevalent in over 71% of US adults¹ and has become one of the most important threats to public health worldwide. Compared to individuals with normal weight, those with obesity, defined as a body mass index (BMI) ≥ 30 kg/m², experience cardiovascular disease (CVD) events at an earlier age and have a shorter average life span.^{2,3} Excess adiposity accelerates atherosclerosis and promotes adverse changes in cardiac structure and function through deleterious effects on the myocardium as well as the vasculature, and through obesity-related comorbidities, including hypertension, dyslipidaemia, and type 2 diabetes mellitus.^{4,5} Although increasing BMI is associated with increasing risk of morbidity and mortality across populations, CVD risk is not uniform for individuals with similar BMI and can vary substantially across sex and racial/ethnic groups. Nonetheless, BMI thresholds continue to guide current clinical diagnosis of obesity and candidacy for interventions with potential to improve CVD outcomes.⁶ Besides BMI, other discriminators of cardiovascular risk are needed in individuals at risk for cardiometabolic disease. Imaging technologies such as computed tomography (CT) can be used to assess body composition and distinguish between fat and lean mass directly *in vivo* via their respective radiodensities, or attenuation, within anatomical compartments.⁷

Recently, intermuscular adipose tissue (IMAT) has emerged as a distinct adipose depot reflecting skeletal muscle (SM) fat infiltration with unique and evolving biological properties. Whereas fatty 'marbling' of meat is commercially valued in livestock, IMAT in humans has been associated with insulin resistance and type 2 diabetes.^{8,9} Intermuscular adipose tissue can be found in most SM groups, and while IMAT increases with BMI, it can vary considerably between individuals. Early reports suggest that IMAT has a proinflammatory secretome with increased expression of interleukin-6 and tumour necrosis factor, which may affect the metabolic function and insulin sensitivity of neighbouring muscle tissue.^{10–12} but the impact of IMAT on CVD events is not well understood.

Coronary microvascular dysfunction (CMD), quantified noninvasively using positron emission tomography (PET) as an impaired global coronary flow reserve (CFR < 2) with normal myocardial perfusion imaging, is independently associated with elevated BMI¹³ and future risk of heart failure (HF), myocardial infarction (MI), and death.^{14–19} It is also associated with residual inflammation and myocardial stiffness independently of conventional CVD risk factors in patients with cardiometabolic disease.^{20–23} We previously demonstrated an independent inverted J-shaped relationship between BMI and CFR such that in obese patients, CFR decreased linearly with increasing BMI (adjusted $P < .0001$).¹³ We found that CMD was prevalent in obese patients, worsened with increasing BMI, and was a better discriminator of CVD risk as compared to BMI. Given the limitations of BMI, we sought to investigate the relationship between IMAT, CMD, and cardiovascular outcomes. We hypothesized that measures of both SM quantity and quality are associated with CMD and modify its effect on CVD events independently of obesity.

Methods

Study population

The study population (see [Supplementary data online, Figure S1](#)) included consecutive patients undergoing cardiac stress testing with PET/CT at Brigham and Women's Hospital (Boston, MA) from 2007 to 2014. The most common indication for PET was the evaluation of chest pain, dyspnoea, or their combination. Patients with known coronary artery disease (CAD), including a history of previous MI or revascularization, clinical HF,

severe valvular disease, PET evidence of flow-limiting CAD (defined as a summed stress score > 2), or abnormal left ventricular ejection fraction (LVEF $< 40\%$) were excluded, as were patients with end-stage disease, including liver, lung, or kidney disease, active malignancy, or planned bariatric surgery at the time of imaging. Medical history, medication use, laboratory findings, height, and weight were ascertained at the time of PET/CT imaging. Body mass index was calculated as the ratio between weight in kilograms and the square of height in metres. The Chronic Kidney Disease Epidemiology Collaboration equation was used to determine estimated glomerular filtration rate (eGFR). The study was approved by the Mass General Brigham Healthcare Institutional Review Board and performed in accordance with institutional guidelines.

Positron emission tomography imaging

Patients were imaged with a whole-body PET/CT scanner (Discovery RX or STE LightSpeed 64, GE Healthcare, Milwaukee, WI) using ⁸²Rb and ¹³N-ammonia as flow radiotracers at rest and following pharmacological stress. Patients were instructed to avoid caffeine or methylxanthine-containing substances 24 h before the scan. Rest LVEF was obtained from gated myocardial perfusion images processed with commercially available software (Corridor4DM, INVIA Medical Imaging Solutions, Ann Arbor, MI). Semi-quantitative visual interpretation was performed using a standard 17-segment, 5-point scoring system to determine summed rest, stress, and difference scores, reflecting scar, ischaemia plus scar, or ischaemia, respectively. Absolute global myocardial blood flow (MBF, mL/min/g) was measured at rest, and peak vasodilator-induced hyperaemia and dynamic images were fitted into a validated two-compartment kinetic model as previously described.²⁴ Coronary flow reserve was obtained as the ratio of global stress to rest MBF.

Computed tomography-derived body composition analysis

Thoracic body composition metrics, including cross-sectional areas (in cm²) of subcutaneous adipose tissue (SAT), SM, and IMAT,²⁵ were measured at the level of the 12th vertebra (T12) on low-dose, non-contrast axial CT images obtained for attenuation correction during cardiac PET/CT imaging using a standard acquisition protocol (tube voltage 120–140 kV, tube current 20–40 mA, exposure time < 2.0 ms, slice thickness 5.0 mm).^{26,27} Studies with artefacts related to patient positioning or image acquisition precluding soft tissue assessment at this level were excluded (see [Supplementary data online, Figure S1](#)). Subcutaneous adipose tissue, SM, and IMAT were quantified using semi-automated threshold-based segmentation in 3DSlicer (version 4.10.1, <https://www.slicer.org/>) by a trained reader (A.S.T.) blinded to study details. Tissue-specific Hounsfield units (HU) were used for SM (–29 to +150 HU) and adipose tissue (–190 to –30 HU) as previously described.^{27,28} Hepatic attenuation (HA, in HU) was obtained by manual tracing of a circular region of interest within the liver parenchyma at the T12 level. Boundaries of each compartment were verified with excellent intrareader class correlations ($\geq .997$). Randomly selected samples were re-segmented by independent readers (J.P.M., F.J.F.) blinded to patient details with excellent interreader class correlations ($\geq .972$). In addition, epicardial adipose tissue (EAT) volume (in cm³) was quantified using a validated automated deep learning segmentation tool²⁹ and confirmed manually by a blinded reader (B.F.) on a subset of 30 attenuation correction CTs with excellent interclass correlation (.97). All body composition analyses were blinded to clinical, PET, and outcomes data.

Outcomes

Patients were followed over a median 5.8 (Q1–Q3 3.2–7.1) years for the occurrence of a primary endpoint composite of death, hospitalization for nonfatal MI, or HF. Time to first event was analysed. Ascertainment of clinical endpoints was determined by blinded committee adjudication of the longitudinal medical record, the Mass General Brigham Healthcare Research Patient Data Registry, the National Death Index, mail surveys, and telephone

calls. To be classified as hospitalization for nonfatal MI or HF, discharge with the corresponding primary diagnosis was required, and only events meeting the universal definition of MI³⁰ or prespecified criteria for clinical signs, symptoms, and escalation of therapy for HF, respectively, were adjudicated as such. All hospitalization events occurred >30 days following PET imaging.

Statistical analyses

Baseline characteristics are presented as rates with percentages for categorical variables and medians with interquartile ranges (Q1–Q3) for continuous variables. We used the Fisher exact test and the Wilcoxon rank-sum test to assess for differences in categorical and continuous baseline characteristics, respectively. Coronary microvascular dysfunction was defined as CFR <2, a prognostically important cutpoint associated with worse cardiovascular outcomes in patients undergoing evaluation for suspected CAD,^{31,32} and approximated the median CFR of the clinical cohort. Spearman's correlation was used to describe the association between the continuous variables of BMI and thoracic body composition metrics SAT, SM, EAT, HA, and IMAT. Fatty muscle fraction (FMF, %) was defined as $IMAT/(SM + IMAT) \times 100$.

Linear regression was used to assess for independent relationships between CFR and body composition metrics. Candidate variables tested included demographic characteristics, medical history and medication use, laboratory findings and noninvasive imaging parameters, with the most clinically important covariates or significant univariable associations included in the multivariable model. To avoid overfitting, demographic and medical history variables (age, sex, anginal symptoms, hypertension, dyslipidaemia, diabetes, tobacco use, family history of premature CAD, BMI >27 kg/m², and oestrogen status) were incorporated into multivariable modelling using a validated pretest clinical risk score for diagnosing CAD (with values 0–8, 9–15, and 16–24 indicating low, intermediate, and high pretest risk, respectively) as previously described.³³ The final multivariable linear regression model for CFR included the pretest clinical score, nonwhite race, BMI, eGFR <60 mL/min/1.73 m², LVEF, SAT, SM, and IMAT (or EAT, or HA or FMF, modelled separately due to high collinearity). These variables were also incorporated into a logistic regression model to quantify the association between FMF and CMD.

Cumulative event-free survival curves for the composite endpoint of death or hospitalization for nonfatal MI or HF were compared across categories of CMD and obesity or IMAT median using the log-rank test. Cox proportional hazards models were used to examine for multivariable-adjusted associations of thoracic body composition, CFR, and events. Univariate associations were tested, and sequential Cox models controlled for effects of clinically important covariates: Model 1 was adjusted for traditional risk factors, including pretest clinical score, race, eGFR, LVEF, and BMI, with sequential addition of body composition metrics and CFR to Models 2 and 3, respectively. Nested models were compared with the likelihood ratio test, and the Akaike information criterion was assessed to avoid overfitting. A linear interaction term for CFR and IMAT or FMF was tested for significance in the final adjusted model. The proportional hazards assumption was confirmed for each model using cumulative martingale residuals. In addition, to understand the relative independent contribution of IMAT compared to alternate thoracic ectopic fat depots on clinical outcomes, we sequentially added HA, EAT, and IMAT or FMF to separate Cox models (A, B, and C, respectively) controlling for the effects of pretest clinical score, LVEF, CFR, and BMI at baseline.

To further investigate the presence of effect modification between CMD and IMAT, Poisson regression was performed to compute adjusted annualized rates of events across categories of CMD and IMAT median after adjustment for pretest clinical score, SM and SAT areas. Model fit was assessed with the goodness-of-fit χ^2 test, with a nonsignificant result indicating adequate fit. A *P*-value of <.05 was considered to indicate statistical significance, and all tests were two sided. Statistical analyses were performed using SAS (version 9.4, SAS Institute Inc., Cary, NC) and SPSS (version 28.0, IBM Corp, Armonk, NY).

Results

Baseline characteristics

The distribution of baseline characteristics is shown in [Table 1](#). The median age of patients in the overall cohort was 62.6 (53.7–71.6) years, 69.8% were women, and 46.2% were nonwhite. Approximately 45.9% of patients were obese (BMI 30–61 kg/m²), with 21.7% of the cohort classified as having class I obesity (BMI 30–34.9 kg/m²), 13.1% as class II obesity (BMI 35–39.9 kg/m²), and 11.1% as class III obesity (BMI ≥40 kg/m²). Hypertension and dyslipidaemia were prevalent comorbidities present in 72.6% and 58.4% of patients, respectively, and 25.6% of patients had diabetes. Median LVEF was 63% (57–69) and 43.0% of patients had CMD, with median CFR of 2.1 (1.7–2.6) reflecting median peak stress and rest MBF values of 2.3 (1.8–2.9) and 1.1 (.8–1.4) mL/min/g, respectively. Compared with the nonobese, obese patients had higher median indices of SAT (248.7 vs. 101.5 cm²), SM (95.6 vs. 78.9 cm²), IMAT (20.4 vs. 6.5 cm², *P* < .001 for all), and similar distributions of CFR. They also had higher median EAT (91.7 vs. 60.9 cm³) and lower HA (51.5 vs. 62.3 HU) consistent with higher liver fat content (*P* < .001 for both). BMI correlated highly with SAT and IMAT (*r* = .84 and .71, respectively, *P* < .001) and moderately with SM (*r* = .52, *P* < .001) ([Figure 1](#); [Supplementary data online, Figure S2](#)). Representative patients of similar demographics and BMI with variable thoracic body composition metrics and CFR values are shown in [Figure 2](#).

Association between thoracic body composition and coronary flow reserve

In univariable linear regression analysis, increasing BMI was inversely associated with CFR [β (se) = $-.07$ (.03), *P* = .04 for +10 kg/m² BMI] as was increasing SAT, IMAT, and EAT, while increasing HA was directly associated with CFR (*P* < .01 for all) ([Table 2](#)). After adjustment for clinical covariates and body composition metrics, decreasing SM and increasing IMAT, but not BMI or SAT, remained independently associated with worse CFR [β (se) = .027 (.013) and $-.047$ (.023), adjusted *P* = .03 and .04 for +10 cm² SM and IMAT areas, respectively] ([Table 2](#)). Findings were confirmed using FMF [β (se) = $-.008$ (.004), adjusted *P* = .02 for +1% FMF]. In univariable- and multivariable-adjusted logistic regression analyses, every 1% increase in FMF was independently associated with a 2% increased odds of CMD [odds ratio (OR) 1.02 (1.01–1.04), unadjusted *P* = .008 and adjusted *P* = .04] defined as CFR < 2.

Thoracic body composition, coronary flow reserve, and adverse events

Over a median follow-up of 5.8 (3.2–7.1) years, 98 patients met the composite endpoint of death and hospitalization for MI or HF, including 54 deaths (see [Supplementary data online, Table S1](#)). In univariable analysis, CFR and IMAT were significantly associated with major adverse events [hazard ratio (HR) 1.81, 95% confidence interval (CI) 1.28–2.56 per -1 U CFR, *P* = .001 and HR 1.21, 95% CI 1.09–1.35 per +10 cm² IMAT, *P* < .001, respectively] ([Table 3](#)). The addition of body composition metrics SAT, SM, and IMAT into a multivariable model of clinically important covariates, including pretest clinical score, race, BMI, eGFR, and LVEF led to improvement in model statistics (global χ^2 65.4 vs. 26.8 for Model 2 vs. Model 1, respectively, *P* < .001), as did the sequential addition of CFR (global χ^2 74.5 vs. 65.4 for Model 3 vs. Model 2, respectively, *P* < .001) ([Table 3](#)). In the final adjusted model, both lower CFR and higher IMAT were associated with increased

Table 1 Baseline characteristics of the study population

Characteristic	Overall (N = 669)	Obese ^a		P-value*
		No (n = 362)	Yes (n = 307)	
Demographics				
Age (years)	62.6 (53.7–71.6)	64.9 (55.1–74.2)	60.1 (52.1–67.1)	<.001
Female (%)	467 (69.8%)	236 (65.2%)	231 (75.2%)	.005
Nonwhite race (%)	309 (46.2%)	146 (40.3%)	163 (53.1%)	.001
Body mass index (BMI, kg/m ²)	29.2 (25.1–34.7)	25.6 (23.1–27.8)	35.4 (32.3–39.8)	<.001
Pretest clinical score ^b	11 (8–14)	11 (8–14)	10 (8–14)	.29
Medical history				
Hypertension (%)	486 (72.6%)	231 (63.8%)	255 (83.1%)	<.001
Dyslipidaemia (%)	391 (58.4%)	202 (55.8%)	189 (61.6%)	.14
Diabetes (%)	171 (25.6%)	57 (15.7%)	114 (37.1%)	<.001
Family history of CAD (%)	195 (29.1%)	89 (24.6%)	106 (34.5%)	.006
Current tobacco use (%)	56 (8.4%)	31 (8.56%)	25 (8.14%)	.89
Medication use				
Aspirin (%)	353 (52.8%)	199 (55.0%)	154 (50.2%)	.24
Beta-blocker (%)	289 (43.2%)	145 (40.1%)	144 (46.9%)	.09
Angiotensin inhibitor (%)	197 (29.4%)	88 (24.3%)	109 (35.5%)	.002
Statin (%)	343 (51.3%)	177 (48.9%)	166 (54.1%)	.19
Oral hypoglycaemic (%)	80 (12.0%)	24 (6.63%)	56 (18.2%)	<.001
Insulin (%)	71 (10.6%)	18 (5.0%)	53 (17.3%)	<.001
Laboratory values				
Creatinine (mg/dL)	.83 (.72–.96)	.84 (.72–.96)	.82 (.70–.95)	.30
eGFR (mL/min/1.73 m ²)	84.3 (70.1–96.7)	82.1 (70.4–93.8)	87.1 (70.2–98.6)	.02
CT body composition measures				
Subcutaneous adipose tissue (SAT, cm ²)	155.4 (92.7–246.8)	101.5 (69.3–139.9)	248.7 (187.9–317.8)	<.001
Skeletal muscle (SM, cm ²)	87.7 (73.5–106.2)	78.9 (67.8–98.7)	95.6 (82.4–114.5)	<.001
Intermuscular adipose tissue (IMAT, cm ²)	11.5 (5.6–22.7)	6.5 (4.0–11.3)	20.4 (13.2–34.2)	<.001
Fatty muscle fraction (FMF, %)	11.6 (6.3–19.1)	7.5 (4.6–12.7)	18.0 (11.7–25.2)	<.001
Epicardial adipose tissue (EAT, cm ³)	74.3 (47.9–113.1)	60.9 (38.5–93.2)	91.7 (59.5–132.5)	<.001
Hepatic attenuation (HA, mean HU)	58.9 (48.9–65.1)	62.3 (56.9–67.8)	51.5 (40.0–60.2)	<.001
PET imaging parameters				
Left ventricular ejection fraction (LVEF, %)	63 (57–69)	63 (57–70)	63 (56–68)	.46
Rest myocardial blood flow (mL/min/g)	1.1 (.8–1.4)	1.1 (.9–1.5)	1.0 (.8–1.3)	<.001
Stress myocardial blood flow (mL/min/g)	2.3 (1.8–2.9)	2.5 (2.0–3.1)	2.1 (1.6–2.6)	<.001
Coronary flow reserve (CFR)	2.1 (1.7–2.6)	2.1 (1.7–2.6)	2.1 (1.6–2.5)	.13
Coronary microvascular dysfunction (CMD, %)	288 (43.0)	151 (41.7)	137 (44.6)	.48

Continuous variables are presented as medians (Q1–Q3) and categorical variables as n, (%).

CAD, coronary artery disease; CT, computed tomography; eGFR, estimated glomerular filtration rate; HU, Hounsfield unit; PET, positron emission tomography.

^aObese is defined as body mass index ≥ 30 .

^bPretest clinical score integrates age, sex, presence of hypertension, dyslipidaemia, diabetes mellitus, body mass index >27 kg/m², oestrogen status, smoking history, family history, and angina history into a pretest probability of CAD in patients presenting for stress imaging with symptoms of suspected CAD. Risk: low (0–8), intermediate (9–15), and high (>15).³³

*The P-value is for the comparison between obese groups and is based on the Fisher exact test for categorical variables and the Wilcoxon rank-sum test for continuous variables.

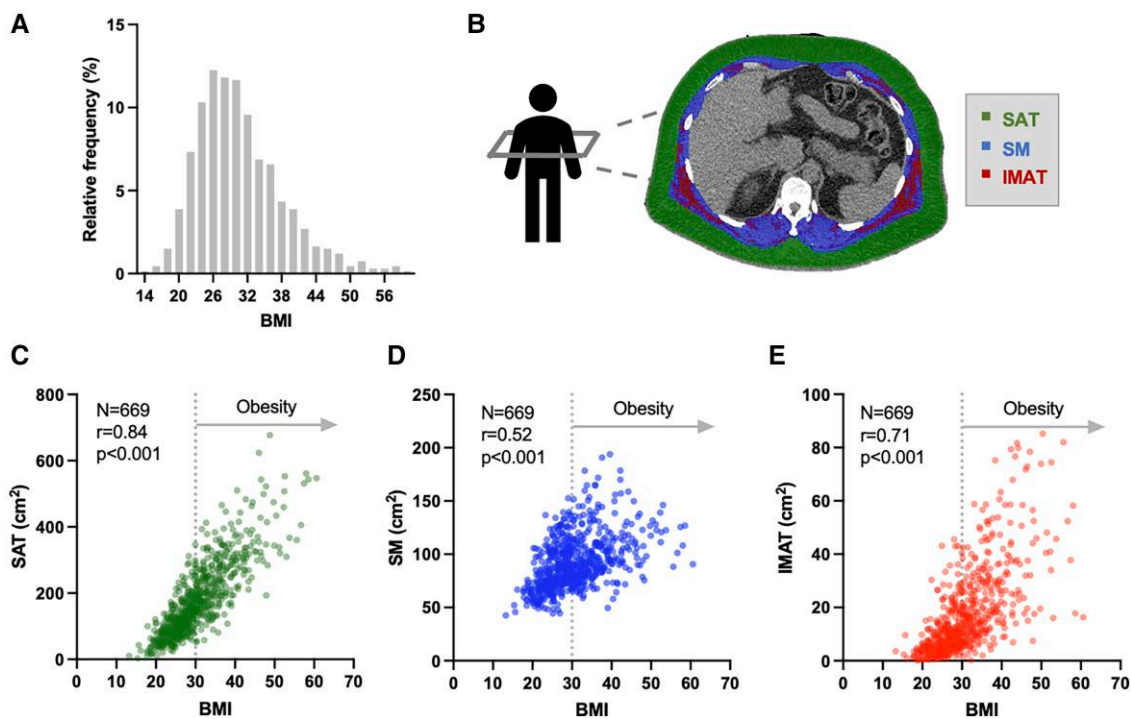


Figure 1 Thoracic body composition compartments and relationship to body mass index. (A) Distribution of body mass index in the study population. (B) Example of computed tomography slice selection at the 12th thoracic vertebra (T12) level and segmentation of subcutaneous adipose tissue (green), skeletal muscle (blue), and intermuscular adipose tissue (red) areas. Relationship between body mass index and subcutaneous adipose tissue (C), skeletal muscle (D), and intermuscular adipose tissue (E)

events [HR 1.78 (1.23–2.58) per -1 U CFR and 1.53 (1.30–1.80) per $+10$ cm² IMAT, adjusted $P = .002$ and $P \leq .0001$, respectively], while higher SM and SAT were protective [HR .89 (.81–.97) per $+10$ cm² SM and .94 (.91–.98) per $+10$ cm² SAT, adjusted $P = .01$ and $P = .003$, respectively]. There was a significant interaction between CFR and IMAT such that patients with both CMD and fatty muscle demonstrated the highest risk of events (adjusted P for interaction = .02). Every 1% increase in FMF conferred an independent 7% increased risk of major adverse events [HR 1.07 (1.04–1.09), adjusted $P < .001$] and modified the effect of CMD on outcomes (adjusted P for interaction = .04).

Intermuscular adiposity compared with alternate thoracic ectopic fat depots

To understand the relative contribution of IMAT compared to alternate thoracic ectopic fat depots on clinical outcomes, we sequentially added HA, EAT, and IMAT or FMF to multivariable-adjusted models controlling for the effects of pretest clinical score, LVEF, CFR, and BMI at baseline. While EAT was associated with increased risk of events in unadjusted or limited adjusted analysis, this association was no longer significant after adjustment for IMAT and other body composition metrics in the presence of CFR (Table 4). In contrast, the highly significant association between IMAT (or FMF) and adverse outcomes was unchanged after further adjustment for other thoracic ectopic fat depots [HR 1.52 (1.27–1.83) per $+10$ cm² IMAT, adjusted $P < .0001$] (Table 4). Our results, including the significant interaction between IMAT (or FMF) and CFR, remained unchanged in expanded multivariable-adjusted

modelling (see Supplementary data online, Table S2). These findings support IMAT as a robust marker of cardiovascular risk, even as compared to more conventional measures of visceral adiposity such as fatty liver and epicardial fat.

Obesity, intermuscular adiposity, coronary microvascular dysfunction, and outcomes

To visualize the impact of effect modification of IMAT on CMD and cardiovascular events, we stratified results by CMD and obesity (Figure 3A and B) or IMAT median (Figure 3C and D). In adjusted analysis, patients with CMD with or without obesity experienced the highest cumulative rate of events (adjusted $P < .001$, Figure 3B). Elevated BMI did not further stratify risk among patients with CMD (Figures 3B and 4A). In contrast, only those patients with both CMD and high IMAT experienced the highest rate of adverse events (adjusted $P < .001$, Figures 3D and 4B), with an adjusted annualized rate of events of 5.1% (adjusted $P = .02$). The presence of both SM fat infiltration and CMD identified a novel at-risk cardiometabolic phenotype independent of conventional measures of adiposity or CVD.

Discussion

In this work, we demonstrate a novel relationship between IMAT, CMD, and cardiovascular outcomes by leveraging advances in non-invasive imaging. First, we found that lower SM quantity and quality were associated with CMD, independently of conventional risk factors.



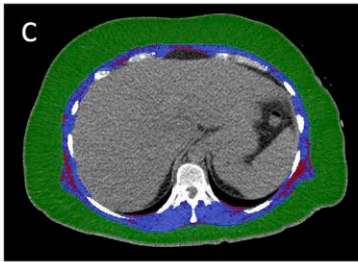
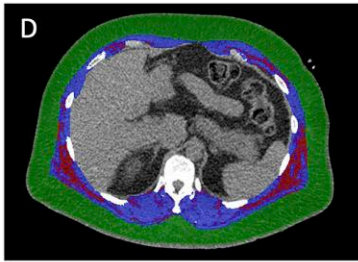
Age	55 years	50 years
Sex	Female	Female
Race	Hispanic	Hispanic
BMI	35.5 kg/m²	36.3 kg/m²
		
		
	SAT 304.5 cm² SM 89.5 cm² IMAT 14.1 cm²	SAT 239.8 cm² SM 110.8 cm² IMAT 29.8 cm²
CFR	2.4	1.4

Figure 2 Characterization of thoracic body composition at the 12th thoracic vertebra (T12) level in representative patients (A/C, B/D) of similar age, sex, race, and body mass index with normal renal function, left ventricular ejection fraction, and myocardial perfusion. Relative to patient (A/C), patient (B/D) demonstrated decreased subcutaneous adipose tissue and increased skeletal muscle and intermuscular adipose tissue areas, also with coronary flow reserve <2, consistent with coronary microvascular dysfunction. Non-annotated images (A, B) appear above the respective segmented ones (C, D). BMI, body mass index; SAT, subcutaneous adipose tissue; SM, skeletal muscle; IMAT, intermuscular adipose tissue; CFR, coronary flow reserve

Table 2 Univariable- and multivariable-adjusted associations with coronary flow reserve

	Univariable β (se)	P-value	Multivariable ^a β (se)	P-value
Pretest clinical score	-.016 (.006)	.01	-.017 (.006)	.008
Nonwhite race	.041 (.051)	.42	.039 (.052)	.46
eGFR < 60 mL/min/1.73 m ²	-.020 (.085)	.81	.063 (.086)	.47
LVEF (+10%)	-.058 (.028)	.04	-.040 (.029)	.17
BMI (+10 kg/m ²)	-.069 (.033)	.04	.005 (.072)	.94
SAT (+10 cm ²)	-.007 (.002)	.003	-.005 (.005)	.32
SM (+10 cm ²)	.014 (.010)	.18	.027 (.013)	.03
IMAT (+10 cm ²)	-.053 (.016)	.001	.047 (.023)	.04
EAT (+10 cm ³)	-.013 (.005)	.005	-.007 (.005)	.15
HA (+10 HU)	.049 (.016)	.003	.039 (.021)	.06
FMF ^b (+1%)	-.011 (.003)	<.0001	-.008 (.004)	.02

β -Estimates with standard error (se) are listed.

BMI, body mass index; CFR, coronary flow reserve; EAT, epicardial adipose tissue; HA, hepatic attenuation; HU, Hounsfield unit; IMAT, intermuscular adipose tissue; SAT, subcutaneous adipose tissue; SM, skeletal muscle; FMF, fatty muscle fraction, IMAT/(SM + IMAT) × 100.

^aAdjusted for pretest clinical score, nonwhite race, eGFR <60 mL/min/1.73 m², LVEF, BMI, SAT, SM, and IMAT or EAT, or HA or FMF. IMAT, EAT, HA, and FMF were highly collinear and separately modelled to avoid overfitting.

^bEvery 1% increase in FMF was independently associated with a 2% increased odds of CMD, defined as CFR <2 [OR 1.02 (1.01–1.04), unadjusted P = .008 and adjusted P = .04].

Table 3 Univariable- and multivariable-adjusted associations with major adverse events

Variable	Univariable		Model 1 ^a (traditional risk factors)		Model 2 ^b (+body composition)		Model 3 ^c (+CFR)	
	HR (95% CI)	P-value	HR (95% CI)	P-value	HR (95% CI)	P-value*	HR (95% CI)	P-value*
	Model statistic		Model statistic		Model statistic		Model statistic	
Global χ^2			26.8	Ref.	65.4	<.001	74.5	<.001
AIC			1157		1129		1121	
Pretest clinical score	1.09 (1.04–1.15)	<.001	1.09 (1.03–1.15)	.001	1.07 (1.01–1.13)	.01	1.06 (1.01–1.12)	.03
Nonwhite race	.99 (.66–1.47)	.95	.97 (.65–1.44)	.86	1.16 (.77–1.74)	.48	1.20 (.80–1.80)	.38
eGFR < 60 mL/min/1.73 m ²	1.99 (1.15–3.45)	.01	1.56 (.89–2.74)	.12	1.37 (.78–2.40)	.27	1.43 (.82–2.50)	.21
LVEF (+10%)	.69 (.56–.86)	.001	.70 (.56–.87)	.001	.72 (.57–.89)	.003	.70 (.56–.87)	.001
BMI (+10 kg/m ²)	.90 (.69–1.18)	.46	.89 (.67–1.18)	.42	1.08 (.60–1.95)	.80	1.06 (.58–1.92)	.85
SAT area (+10 cm ²)	.98 (.96–1.00)	.078			.94 (.91–.98)	.003	.94 (.91–.98)	.003
SM area (+10 cm ²)	.98 (.90–1.10)	.60			.88 (.80–.96)	.006	.89 (.81–.97)	.01
IMAT area (+10 cm ²)	1.21 (1.09–1.35)	<.001			1.59 (1.35–1.86)	<.001	1.53 (1.30–1.80)	<.0001
Coronary flow reserve (–1 U)	1.81 (1.28–2.56)	.001					1.78 (1.23–2.58)	.002
							+Interaction (IMAT × CFR)	.02
Fatty muscle fraction (+1%)	1.04 (1.02–1.06)	<.0001			1.07 (1.05–1.10)	<.001	1.07 (1.04–1.09)	<.001
							+Interaction (FMF × CFR)	.04

Major adverse events include death and hospitalization for nonfatal myocardial infarction or heart failure.

CFR, coronary flow reserve; eGFR, estimated glomerular filtration rate; LVEF, left ventricular ejection fraction; BMI, body mass index; SAT, subcutaneous adipose tissue; SM, skeletal muscle; IMAT, intermuscular adipose tissue; FMF, fatty muscle fraction; HR, hazard ratio; CI, confidence interval.

^aAdjusted for pretest clinical score (includes age, sex, hypertension, dyslipidaemia, diabetes, family history of premature CAD, tobacco use, anginal symptoms, oestrogen status, and presence of BMI ≥ 27 kg/m²), race, eGFR, LVEF, and BMI.

^bAdjusted for pretest clinical score, race, eGFR, LVEF, BMI, and body composition metrics (SAT, SM, IMAT, or FMF).

^cAdjusted for pretest clinical score, race, eGFR, LVEF, BMI, body composition metrics (SAT, SM, IMAT, or FMF), and CFR.

*P-value for likelihood ratio test between sequential models; AIC, Akaike information criterion, lower value indicates better model fit.

Table 4 Sequential addition of thoracic ectopic fat depots to multivariable-adjusted models for major adverse events

Variable	Univariable		Model A ^a (+HA)		Model B ^b (+EAT)		Model C ^c (+IMAT)	
	HR (95% CI)	P-value	HR (95% CI)	P-value	HR (95% CI)	P-value	HR (95% CI)	P-value
AIC			1144		1135		1118	
BMI (+10 kg/m ²)	.90 (.69–1.18)	.46	1.54 (.87–2.73)	.14	1.34 (.73–2.43)	.34	.99 (.54–1.82)	.96
SAT area (+10 cm ²)	.98 (.96–1.00)	.08	.96 (.92–.99)	.03	.96 (.92–.99)	.04	.95 (.91–.99)	.02
SM area (+10 cm ²)	.98 (.90–1.10)	.60	.92 (.83–1.02)	.10	.92 (.83–1.01)	.08	.90 (.82–.99)	.03
HA (+10 HU)	1.01 (.88–1.15)	.90	.98 (.82–1.16)	.77	1.06 (.88–1.27)	.54	1.18 (.97–1.43)	.09
EAT volume (+10 cm ³)	1.06 (1.03–1.09)	<.001			1.07 (1.03–1.11)	.0004	1.04 (1.00–1.08)	.06
IMAT area (+10 cm ²)	1.21 (1.09–1.35)	<.001					1.52 (1.27–1.83)	<.0001
Fatty muscle fraction (+1%)	1.04 (1.02–1.06)	<.0001					1.06 (1.03–1.09)	<.0001

Major adverse events include death and hospitalization for nonfatal myocardial infarction or heart failure.

HA, hepatic attenuation; EAT, epicardial adipose tissue; IMAT, intermuscular adipose tissue; AIC, Akaike information criterion (lower value indicates better model fit); HR, hazard ratio; CI, confidence interval; BMI, body mass index; SAT, subcutaneous adipose tissue; SM, skeletal muscle; HU, Hounsfield unit; FMF, fatty muscle fraction; LVEF, left ventricular ejection fraction; CFR, coronary flow reserve.

^aAdjusted for pretest clinical score (includes age, sex, hypertension, dyslipidaemia, diabetes, family history of premature CAD, tobacco use, anginal symptoms, oestrogen status, and presence of BMI ≥ 27 kg/m²), LVEF, CFR, BMI, SAT, SM, and HA.

^bAdjusted for pretest clinical score, LVEF, CFR, BMI, SAT, SM, HA, and EAT.

^cAdjusted for pretest clinical score, LVEF, CFR, BMI, SAT, SM, HA, EAT, and IMAT or FMF.

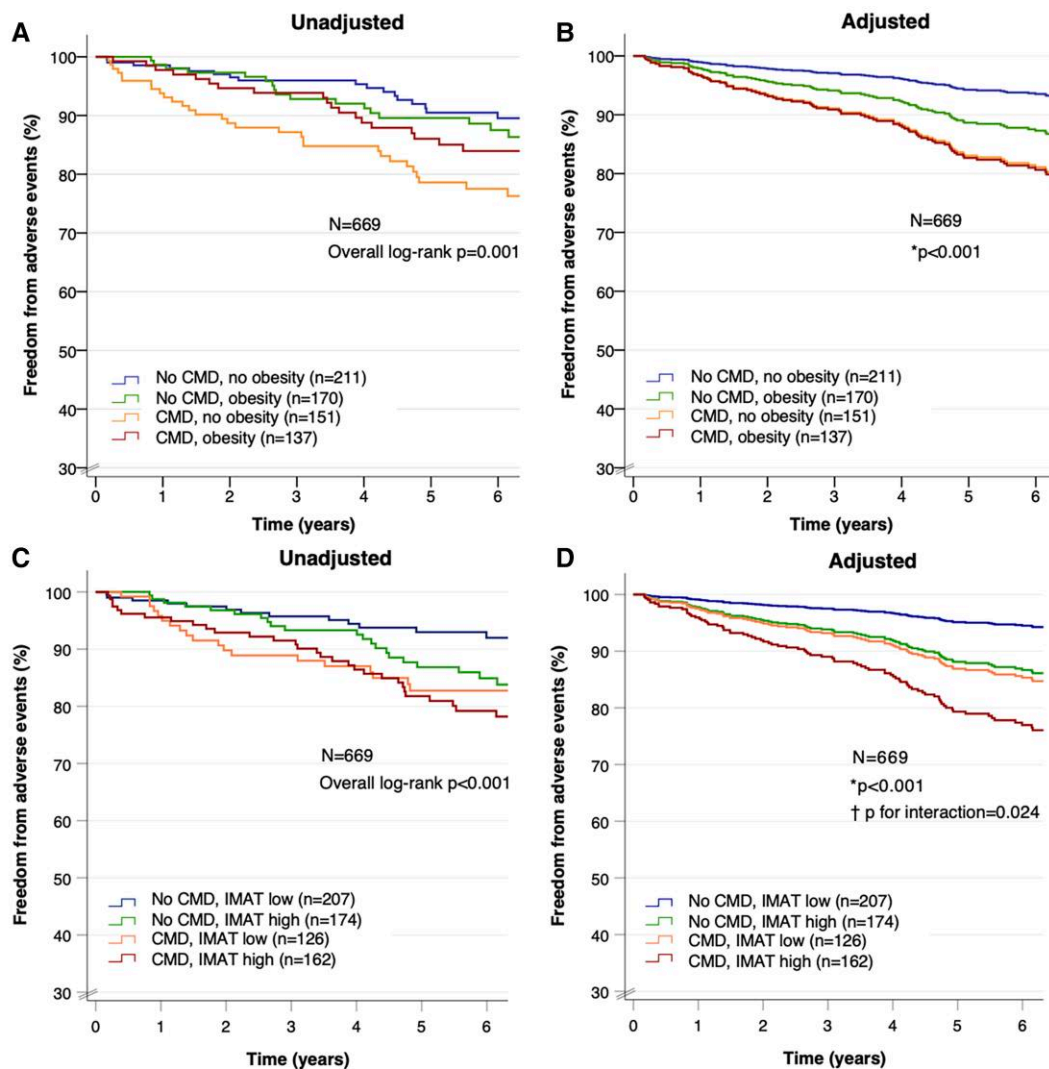


Figure 3 Unadjusted (A, C) and adjusted (B, D) freedom from major adverse events by coronary microvascular dysfunction and obesity (A, B) or intermuscular adipose tissue median (C, D). Major adverse events include death and hospitalization for nonfatal myocardial infarction or heart failure. CMD, coronary microvascular dysfunction, coronary flow reserve <2 ; obesity, body mass index ≥ 30 ; IMAT, intermuscular adipose tissue, high ≥ 11.5 cm^2 . Asterisk: adjusted for pretest clinical score, race, estimated glomerular filtration rate <60 , left ventricular ejection fraction, skeletal muscle, and subcutaneous adipose tissue areas. Dagger: P -value refers to interaction between coronary flow reserve and intermuscular adipose tissue continuous variables

Every 1% increase in FMF conferred an independent 2% increased odds of CMD. Second, in adjusted analyses for outcomes, we showed that both higher IMAT and lower CFR were associated with increased risk of CVD events, while higher SM and SAT were protective. Every 1% increase in FMF conferred a 7% increased risk of CVD events. Third, the presence of elevated IMAT, not BMI, modified the effect of CMD on outcomes such that patients with both CMD and fatty muscle, not obesity *per se*, demonstrated the highest risk of CVD events. Fourth, these findings were independent of other conventional thoracic ectopic fat depots and were notably informative for identifying cardiometabolic risk in patients without traditional visceral adiposity. Our data support that thoracic SM quantity and quality are tied to coronary microvascular function and together identify a novel at-risk cardiometabolic phenotype (*Structured Graphical Abstract*).

These findings may be especially relevant for the common clinical demographic represented here, namely patients with ischaemia and no obstructive CAD (INOCA).³⁴ Obesity-related CVD risk is not well captured by BMI, especially in women.³⁵ While increased thoracic IMAT was independently associated with worse CVD events, higher thoracic SM and, to a lesser extent, SAT demonstrated a protective effect. This underscores that, especially in INOCA patients, assessments of BMI and traditional adiposity—which largely reflect lower-risk SAT—are likely to be *insufficient* to appropriately stratify CVD risk. Our findings are clinically relevant and may help to better discern CVD risk among otherwise similar patients, especially younger, female individuals with fewer traditional risk factors and high prevalence of overweight or obesity. *Figure 2A/C and B/D* demonstrate thoracic body composition results in two middle-aged Hispanic women with class II obesity. Despite similar age and BMI, normal renal function,

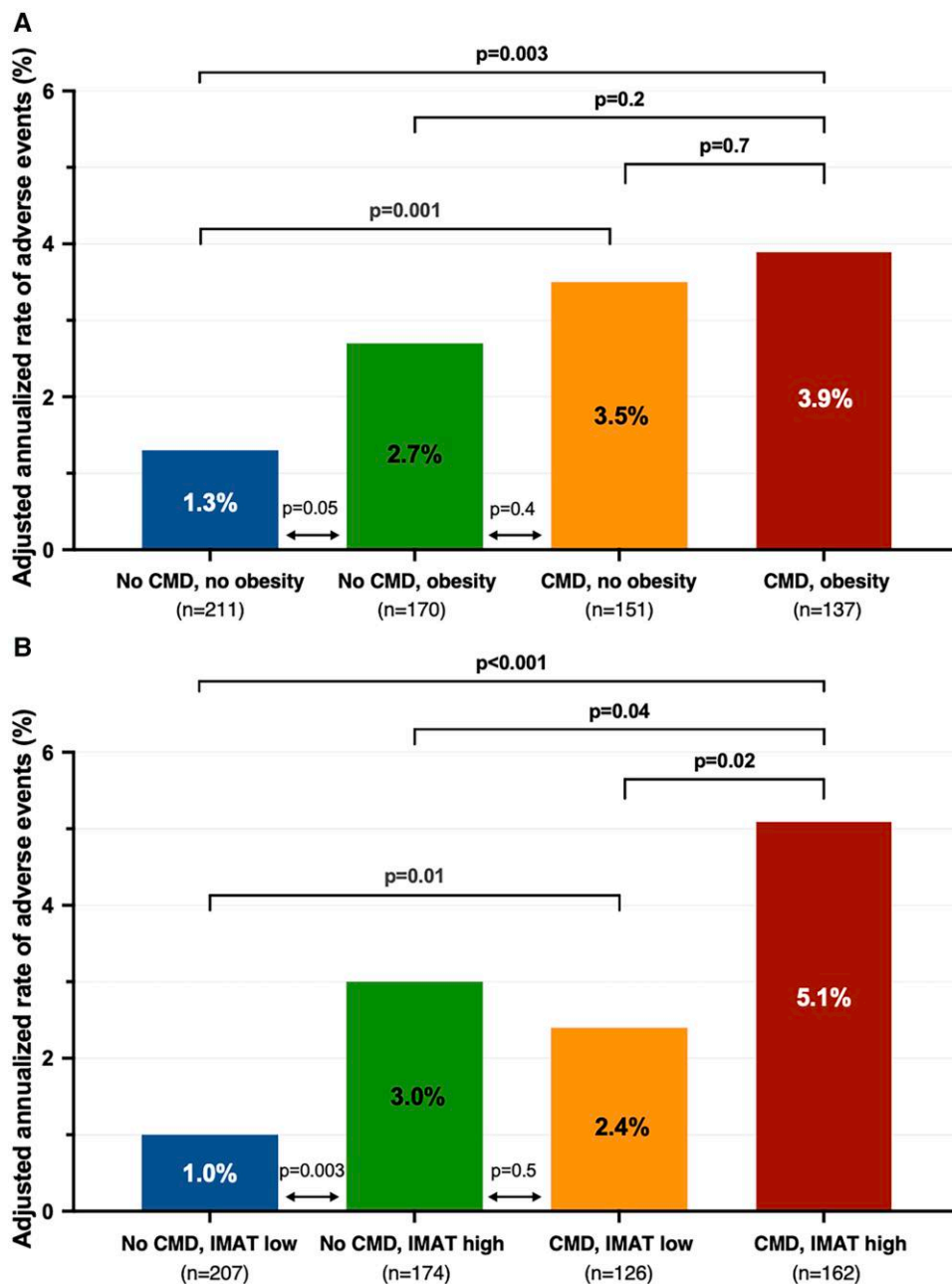


Figure 4 Adjusted annualized rate of major adverse events by coronary microvascular dysfunction and obesity (A) or intermuscular adipose tissue median (B). Major adverse events include death and hospitalization for nonfatal myocardial infarction or heart failure. Poisson regression was adjusted for pretest clinical score, skeletal muscle, and subcutaneous adipose tissue areas. CMD, coronary microvascular dysfunction, coronary flow reserve <2; obesity, body mass index ≥ 30 ; IMAT, intermuscular adipose tissue, high $\geq 11.5 \text{ cm}^2$

LVEF, and myocardial perfusion, patient (B/D) has increased IMAT and decreased CFR as compared to patient (A/C) and thus is at significantly increased risk of CVD events. These findings are relevant for ongoing studies investigating cardiovascular effects of fat and lean weight-modifying glucagon-like peptide-1 receptor agonist therapies. For example, it is possible that perceived lean muscle mass loss in response to incretin-based therapies may involve loss of IMAT resulting in improved skeletal muscle quality.³⁶

Recently described, IMAT reflects an ectopic adipose tissue depot that is interspersed among SM fibres residing within the boundary of

the muscle fascia.⁹ Considered a marker of overall muscle quality, it has been associated with systemic inflammation, insulin resistance, the metabolic syndrome, and coronary artery calcification in a manner comparable to visceral adipose tissue.^{12,37,38} We previously reported on the independent associations between residual inflammation, abnormal CFR, and impaired myocardial strain in a cohort of clinical trial patients with cardiometabolic disease and otherwise well-controlled CVD risk factors and preserved cardiac function.²⁰ We found that individuals with impaired CFR demonstrated the strongest association between markers of HF and inflammation,

building on prior work identifying abnormal global CFR and CMD as robust markers of future risk of HF hospitalization in patients with preserved LVEF.^{15–17} Heart failure with preserved ejection fraction (HFpEF) is prevalent in obese patients and often preceded by exercise intolerance, which may reflect limitations in SM related to functional and structural impairments also common to the myocardium, including reduced oxidative capacity, microvascular dysfunction, capillary rarefaction, and fibrosis.^{39–41} Using a deep learning model for abdominal body composition analysis, we showed that deficient skeletal muscularity but not excess conventional adiposity was independently associated with CMD and future adverse events, especially HF,⁴² in patients with no obstructive CAD. In particular, a sarcopenic CMD phenotype in these female-predominant patients with normal or elevated BMI was associated with the highest CVD risk. Reduced lean body mass, as part of a distinct yet poorly understood SM pathology, has been hypothesized to be a sex-specific contributor to the pathophysiology of HFpEF,⁴³ and CMD and IMAT may help to mediate this effect.

The expansion of IMAT is thought to promote an adverse muscle phenotype associated with metabolic derangements, including impaired bioenergetics, mitochondrial dysfunction, and increased catabolism with loss of lean muscle mass.⁹ Emerging data suggest that the human IMAT secretome is highly immunogenic and inflammatory relative to that of SAT or even VAT depots in individuals with obesity, and may alter immune cell trafficking to neighbouring muscle in a manner that may be critical to regional glucose homeostasis.¹² Taken together, these findings support the hypothesis that common systemic factors involving inflammation and altered glucose metabolism may promote parallel insults to myocardial and SM beds, which may manifest as microvascular dysfunction and intramuscular fat infiltration, respectively, and ultimately contribute to adverse CVD events, including myocardial injury and HFpEF outcomes.

Our study has important limitations including its observational, single-centre design. Despite the use of multivariable-adjusted models, confirmatory and sensitivity testing showing robust data results, residual confounding may persist. Although we leveraged low-dose CTs routinely obtained with clinical cardiac PET studies for the purpose of attenuation correction, we demonstrate excellent segmentation quality assurance, and the ability to obtain concurrent imaging in these patients represents an important strength of this study. Because these were thoracic studies, we focused our cross-sectional assessments at the level of T12 for thoracic body composition analysis. As such, results may differ when compared to abdominal body composition results obtained from the lumbar spine level,^{42,44} and abdominal visceral adipose tissue could not be quantified (although we would expect it to have a less important role in this female-predominant cohort since women have significantly lower visceral and higher subcutaneous adiposity as compared with men³⁵). Since cardiac PET is performed using vasodilator stress, no exercise testing results were available. As only patients with normal visual myocardial perfusion and no evidence of flow-limiting CAD were included, findings are generalizable to an INOCA population. Relative to less accurate or more cumbersome methods for body composition analysis,⁴⁵ opportunistic CT used in this manner may provide personalized prognostic information without added cost or radiation exposure and is poised to grow with rapid developments in artificial intelligence and machine learning. Future studies assessing the impact of therapeutic strategies such as supervised exercise and nutritional, medical, and/or surgical weight loss interventions on SM quality and CMD outcomes are warranted.

Conclusions

In patients without flow-limiting CAD, increased intermuscular adiposity is associated with CMD and adverse cardiovascular outcomes independently of BMI and conventional ectopic fat depots and risk factors. The presence of CMD and SM fat infiltration identified a novel at-risk cardiometabolic phenotype.

Supplementary data

Supplementary data are available at *European Heart Journal* online.

Declarations

Disclosure of Interest

B.F. reports research grants from the National Institutes of Health, AstraZeneca, and Ionis. R.B. reports research grants from Novartis, Amgen, Heartflow and Nanox AI and consulting fees from Heartflow, Nanox AI and Caristo. S.Do. reports research grants from Pfizer, Attralus, GE Healthcare and Siemens and consulting fees from Pfizer. M.F.D.C. reports research grants from Alnylam Pharmaceuticals, Intellia, Gilead Sciences, Sun Pharma, and Xylocor and consulting fees from Valo Health and MedTrace. M.T.L. reports research grants from the National Academy of Medicine, the National Institutes of Health, the American Heart Association, AstraZeneca, Ionis, Johnson & Johnson Innovation, Kowa Pharmaceuticals, and the Risk Management Foundation of the Harvard Medical Institutions. F.J.F. reports research grants from Pfizer, consulting fees from Boston Scientific and holds a related patent (US11322259B2, WO2019051358A1). All other authors report no relevant disclosures.

Data Availability

Data may be shared in a deidentified and anonymized format for use as approved by the independent review board and according to federal and institutional regulations.

Funding

This research was supported by a Lemann Foundation Cardiovascular Research Postdoctoral Fellowship (A.C.A.H.S.) and the Gilead Sciences Research Scholars Program in Cardiovascular Disease and NIH K23HL135438 (V.R.T.).

Ethical Approval

The study was approved by the Mass General Brigham Healthcare Institutional Review Board and performed in accordance with institutional guidelines.

Pre-registered Clinical Trial Number

None supplied.

References

1. Tsao CW, Aday AW, Almarzooq ZI, Anderson CAM, Arora P, Avery CL, et al. Heart disease and stroke statistics—2023 update: a report from the American Heart Association. *Circulation* 2023;**147**:e93–621. <https://doi.org/10.1161/CIR.0000000000001123>
2. Powell-Wiley TM, Poirier P, Burke LE, Despres JP, Gordon-Larsen P, Lavie CJ, et al. Obesity and cardiovascular disease: a scientific statement from the American Heart Association. *Circulation* 2021;**143**:e984–1010. <https://doi.org/10.1161/CIR.0000000000000973>

3. Khan SS, Ning H, Wilkins JT, Allen N, Carnethon M, Berry JD, et al. Association of body mass index with lifetime risk of cardiovascular disease and compression of morbidity. *JAMA Cardiol* 2018;**3**:280–7. <https://doi.org/10.1001/jamacardio.2018.0022>
4. Kenchaiah S, Evans JC, Levy D, Wilson PW, Benjamin EJ, Larson MG, et al. Obesity and the risk of heart failure. *N Engl J Med* 2002;**347**:305–13. <https://doi.org/10.1056/NEJMoa020245>
5. McGill HC Jr, McMahan CA, Herderick EE, Zieske AW, Malcom GT, Tracy RE, et al. Obesity accelerates the progression of coronary atherosclerosis in young men. *Circulation* 2002;**105**:2712–8. <https://doi.org/10.1161/01.CIR.0000018121.67607.CE>
6. Virani SS, Newby LK, Arnold SV, Bittner V, Brewer LC, Demeter SH, et al. 2023 AHA/ACC/ASCP/ASPC/NLA/PCNA guideline for the management of patients with chronic coronary disease: a report of the American Heart Association/American College of Cardiology Joint Committee on Clinical Practice Guidelines. *Circulation* 2023;**148**:e9–119. <https://doi.org/10.1161/CIR.0000000000001168>
7. Shen W, Punyanitya M, Wang Z, Gallagher D, St-Onge MP, Albu J, et al. Total body skeletal muscle and adipose tissue volumes: estimation from a single abdominal cross-sectional image. *Journal of applied physiology* 2004;**97**:2333–8. <https://doi.org/10.1152/jappphysiol.00744.2004>
8. Goodpaster BH, Krishnaswami S, Resnick H, Kelley DE, Haggerty C, Harris TB, et al. Association between regional adipose tissue distribution and both type 2 diabetes and impaired glucose tolerance in elderly men and women. *Diabetes Care* 2003;**26**:372–9. <https://doi.org/10.2337/diacare.26.2.372>
9. Goodpaster BH, Bergman BC, Brennan AM, Sparks LM. Intermuscular adipose tissue in metabolic disease. *Nat Rev Endocrinol* 2022;**19**:285–98. <https://doi.org/10.1038/s41574-022-00784-2>
10. Li M, Wu H, Wang T, Xia Y, Jin L, Jiang A, et al. Co-methylated genes in different adipose depots of pig are associated with metabolic, inflammatory and immune processes. *Int J Biol Sci* 2012;**8**:831–7. <https://doi.org/10.7150/ijbs.4493>
11. Sachs S, Zarini S, Kahn DE, Harrison KA, Perreault L, Phang T, et al. Intermuscular adipose tissue directly modulates skeletal muscle insulin sensitivity in humans. *Am J Physiol Endocrinol Metab* 2019;**316**:E866–E79. <https://doi.org/10.1152/ajpendo.00243.2018>
12. Kahn D, Macias E, Zarini S, Garfield A, Zemski Berry K, Gerszten R, et al. Quantifying the inflammatory secretome of human intermuscular adipose tissue. *Physiol Rep* 2022;**10**:e15424. <https://doi.org/10.14814/phy2.15424>
13. Bajaj NS, Osborne MT, Gupta A, Tavakkoli A, Bravo PE, Vita T, et al. Coronary microvascular dysfunction and cardiovascular risk in obese patients. *J Am Coll Cardiol* 2018;**72**:707–17. <https://doi.org/10.1016/j.jacc.2018.05.049>
14. Taqueti VR, Everett BM, Murthy VL, Gaber M, Foster CR, Hainer J, et al. Interaction of impaired coronary flow reserve and cardiomyocyte injury on adverse cardiovascular outcomes in patients without overt coronary artery disease. *Circulation* 2015;**131**:528–35. <https://doi.org/10.1161/CIRCULATIONAHA.114.009716>
15. Taqueti VR, Solomon SD, Shah AM, Desai AS, Groarke JD, Osborne MT, et al. Coronary microvascular dysfunction and future risk of heart failure with preserved ejection fraction. *Eur Heart J* 2018;**39**:840–9. <https://doi.org/10.1093/eurheartj/ehx721>
16. Taqueti VR, Shaw LJ, Cook NR, Murthy VL, Shah NR, Foster CR, et al. Excess cardiovascular risk in women relative to men referred for coronary angiography is associated with severely impaired coronary flow reserve, not obstructive disease. *Circulation* 2017;**135**:566–77. <https://doi.org/10.1161/CIRCULATIONAHA.116.023266>
17. Taqueti VR, Hachamovitch R, Murthy VL, Naya M, Foster CR, Hainer J, et al. Global coronary flow reserve is associated with adverse cardiovascular events independently of luminal angiographic severity and modifies the effect of early revascularization. *Circulation* 2015;**131**:19–27. <https://doi.org/10.1161/CIRCULATIONAHA.114.011939>
18. Zhou W, Brown JM, Bajaj NS, Chandra A, Divakaran S, Weber B, et al. Hypertensive coronary microvascular dysfunction: a subclinical marker of end organ damage and heart failure. *Eur Heart J* 2020;**41**:2366–75. <https://doi.org/10.1093/eurheartj/ehaa191>
19. Vita T, Murphy DJ, Osborne MT, Bajaj NS, Keraliya A, Jacob S, et al. Association between nonalcoholic fatty liver disease at CT and coronary microvascular dysfunction at myocardial perfusion PET/CT. *Radiology* 2019;**291**:330–7. <https://doi.org/10.1148/radiol.2019181793>
20. Taqueti VR, Shah AM, Everett BM, Pradhan AD, Piazza G, Bibbo C, et al. Coronary flow reserve, inflammation, and myocardial strain: the CIRT-CFR trial. *JACC Basic Transl Sci* 2023;**8**:141–51. <https://doi.org/10.1016/j.jacbts.2022.08.009>
21. Taqueti VR, Ridker PM. Inflammation, coronary flow reserve, and microvascular dysfunction: moving beyond cardiac syndrome X. *JACC Cardiovasc Imaging* 2013;**6**:668–71. <https://doi.org/10.1016/j.jcmg.2013.02.005>
22. Osborne MT, Bajaj NS, Taqueti VR, Gupta A, Bravo PE, Hainer J, et al. Coronary microvascular dysfunction identifies patients at high risk of adverse events across cardiometabolic diseases. *J Am Coll Cardiol* 2017;**70**:2835–7. <https://doi.org/10.1016/j.jacc.2017.09.1104>
23. Shah NR, Cheezum MK, Veeranna V, Horgan SJ, Taqueti VR, Murthy VL, et al. Ranolazine in symptomatic diabetic patients without obstructive coronary artery disease: impact on microvascular and diastolic function. *J Am Heart Assoc* 2017;**6**:e005027. <https://doi.org/10.1161/JAHA.116.005027>
24. El Fakhri G, Kardan A, Sitek A, Dorbala S, Abi-Hatem N, Lahoud Y, et al. Reproducibility and accuracy of quantitative myocardial blood flow assessment with (82)Rb PET: comparison with (13)N-ammonia PET. *J Nucl Med* 2009;**50**:1062–71. <https://doi.org/10.2967/jnumed.104.007831>
25. Tan L, Ji G, Bao T, Fu H, Yang L, Yang M. Diagnosing sarcopenia and myosteatosis based on chest computed tomography images in healthy Chinese adults. *Insights Imaging* 2021;**12**:163. <https://doi.org/10.1186/s13244-021-01106-2>
26. Fuchs G, Chretien YR, Mario J, Do S, Eikermann M, Liu B, et al. Quantifying the effect of slice thickness, intravenous contrast and tube current on muscle segmentation: implications for body composition analysis. *Eur Radiol* 2018;**28**:2455–63. <https://doi.org/10.1007/s00330-017-5191-3>
27. Troschel AS, Troschel FM, Fuchs G, Marquardt JP, Ackman JB, Yang K, et al. Significance of acquisition parameters for adipose tissue segmentation on CT images. *AJR Am J Roentgenol* 2021;**217**:177–85. <https://doi.org/10.2214/AJR.20.23280>
28. Bridge CP, Best TD, Wrobel MM, Marquardt JP, Magudia K, Javidan C, et al. A fully automated deep learning pipeline for multi-vertebral level quantification and characterization of muscle and adipose tissue on chest CT scans. *Radiol Artif Intell* 2022;**4**:e210080. <https://doi.org/10.1148/ryai.210080>
29. Foldyna B, Zeleznik R, Eslami P, Mayrhofer T, Ferencik M, Bittner DO, et al. Epicardial adipose tissue in patients with stable chest pain: insights from the PROMISE trial. *JACC Cardiovasc Imaging* 2020;**13**:2273–5. <https://doi.org/10.1016/j.jcmg.2020.05.024>
30. Thygesen K, Alpert JS, Jaffe AS, Chaitman BR, Bax JJ, Morrow DA, et al. Fourth universal definition of myocardial infarction (2018). *Circulation* 2018;**138**:e618–51. <https://doi.org/10.1161/CIR.0000000000000617>
31. Ong P, Camici PG, Beltrame JF, Crea F, Shimokawa H, Sechtem U, et al. International standardization of diagnostic criteria for microvascular angina. *Int J Cardiol* 2018;**250**:16–20. <https://doi.org/10.1016/j.ijcard.2017.08.068>
32. Taqueti VR, Carli D, F M. Coronary microvascular disease pathogenic mechanisms and therapeutic options: JACC state-of-the-art review. *J Am Coll Cardiol* 2018;**72**:2625–41. <https://doi.org/10.1016/j.jacc.2018.09.042>
33. Morise AP, Haddad WJ, Beckner D. Development and validation of a clinical score to estimate the probability of coronary artery disease in men and women presenting with suspected coronary disease. *Am J Med* 1997;**102**:350–6. [https://doi.org/10.1016/S0002-9343\(97\)00086-7](https://doi.org/10.1016/S0002-9343(97)00086-7)
34. Reynolds HR, Merz B, Berry CN, Samuel C, Saw R, Smilowitz J, et al. Coronary arterial function and disease in women with no obstructive coronary arteries. *Circ Res* 2022;**130**:529–51. <https://doi.org/10.1161/CIRCRESAHA.121.319892>
35. Kammerlander AA, Lyass A, Mahoney TF, Massaro JM, Long MT, Vasari RS, et al. Sex differences in the associations of visceral adipose tissue and cardiometabolic and cardiovascular disease risk: the Framingham Heart Study. *J Am Heart Assoc* 2021;**10**:e019968. <https://doi.org/10.1161/JAHA.120.019968>
36. Taqueti VR, Shaw LJ. Semaglutide and cardiovascular outcomes. *N Engl J Med* 2024;**390**:766. <https://doi.org/10.1056/NEJMc2400414>
37. Yim JE, Heshka S, Albu J, Heymsfield S, Kuznia P, Harris T, et al. Intermuscular adipose tissue rivals visceral adipose tissue in independent associations with cardiovascular risk. *Int J Obes* 2007;**31**:1400–5. <https://doi.org/10.1038/sj.jjo.0803621>
38. Terry JG, Shay CM, Schreiner PJ, Jacobs DR Jr, Sanchez OA, Reis JP, et al. Intermuscular adipose tissue and subclinical coronary artery calcification in midlife: the CARDIA study (Coronary Artery Risk Development in Young Adults). *Arterioscler Thromb Vasc Biol* 2017;**37**:2370–8. <https://doi.org/10.1161/ATVBAHA.117.309633>
39. Mohammed SF, Hussain S, Mirzoyev SA, Edwards WVD, Maleszewski JJ, Redfield MM. Coronary microvascular rarefaction and myocardial fibrosis in heart failure with preserved ejection fraction. *Circulation* 2015;**131**:550–9. <https://doi.org/10.1161/CIRCULATIONAHA.114.009625>
40. Pandey A, LaMonte M, Klein L, Ayers C, Psaty BM, Eaton CB, et al. Relationship between physical activity, body mass index, and risk of heart failure. *J Am Coll Cardiol* 2017;**69**:1129–42. <https://doi.org/10.1016/j.jacc.2016.11.081>
41. Molina AJ, Bharadwaj MS, Van Horn C, Nicklas BJ, Lyles MF, Eggebeen J, et al. Skeletal muscle mitochondrial content, oxidative capacity, and Mfn2 expression are reduced in older patients with heart failure and preserved ejection fraction and are related to exercise intolerance. *JACC Heart Fail* 2016;**4**:636–45. <https://doi.org/10.1016/j.jchf.2016.03.011>
42. Souza A, Rosenthal MH, Moura FA, Divakaran S, Osborne MT, Hainer J, et al. Body composition, coronary microvascular dysfunction, and future risk of cardiovascular events including heart failure. *JACC Cardiovasc Imaging* 2024;**17**:179–91. <https://doi.org/10.1016/j.jcmg.2023.07.014>
43. Diaz-Canestro C, Pentz B, Sehgal A, Yang R, Xu A, Montero D. Lean body mass and the cardiovascular system constitute a female-specific relationship. *Sci Transl Med* 2022;**14**:eabo2641. <https://doi.org/10.1126/scitranslmed.abo2641>
44. Derstine BA, Holcombe SA, Ross BE, Wang NC, Su GL, Wang SC. Skeletal muscle cut-off values for sarcopenia diagnosis using T10 to L5 measurements in a healthy US population. *Sci Rep* 2018;**8**:11369. <https://doi.org/10.1038/s41598-018-29825-5>
45. Zhang L, Bartz TM, Santanasto A, Djousse L, Mukamal KJ, Forman DE, et al. Body composition and incident heart failure in older adults: results from 2 prospective cohorts. *J Am Heart Assoc* 2022;**11**:e023707. <https://doi.org/10.1161/JAHA.121.023707>